Structure of Amorphous Platinum Uridine Green Sulfate by AWAXS and EXAFS

Ritva Serimaa,*,† Veli Eteläniemi,† Tarja Laitalainen,‡ Arthur Bienenstock,§ Sakari Vahvaselkä,† and Timo Paakkari†

Department of Physics, University of Helsinki, P.O. Box 9, Helsinki, FIN-00014 Finland, Department of Chemistry, University of Helsinki, P.O. Box 55, Helsinki, FIN-00014 Finland, and Stanford Synchrotron Radiation Laboratory, Slac Bin 69, P.O. Box 4349, Stanford, California 94305

Received September 25, 1996[⊗]

Amorphous platinum uridine green sulfate was studied using anomalous wide-angle X-ray scattering and X-ray absorption techniques. Experiments were made with synchrotron radiation in the vicinity of the Pt L_{III} absorption edge. The experimental results agree with a mixture model where the major components are mono- and dinuclear Pt complexes. The intramolecular Pt−Pt distance of 3 Å and the shortest intermolecular Pt−Pt distances of 5.1 and 7.3 Å were determined from the approximative regularized Pt−Pt partial radial distribution function. The shortest average Pt−O and Pt−N distance of 2.03 Å was obtained from the EXAFS data.

1. Introduction

Platinum pyrimidine blues[1,2] are antitumor active, amorphous and paramagnetic products formed in reactions of cisplatin or *cis*-diaquadiammineplatinum(II) with pyrimidine bases. In several studies, e.g.,[3−7] products with varying antitumor activities, elemental compositions, and colors have been obtained. Both the detailed structures and the origin of the antitumor activity of platinum pyrimidine blues are unknown.

The binding of pyrimidine bases with diammineplatinum(II) has been studied extensively by synthesizing crystalline model Pt complexes with varying Pt nuclearities.[8−10] The first single-crystal X-ray diffraction study of the tetranuclear mixed-valent Pt complex *cis*-diammineplatinum α-pyridone blue created a basis for understanding the structures and properties of Pt blues.[11,12] On the other hand, the interactions of Pt complexes with DNA have been studied extensively.[13−19]

Structural studies on amorphous Pt blues have been made using EXAFS,[20,21] wide-angle X-ray scattering (WAXS),[6,22−24] and anomalous wide-angle X-ray scattering (AWAXS)[25] methods. In this work the solid state structure of biologically active amorphous platinum uridine green sulfate[6] was studied by means of AWAXS and EXAFS methods.

The closest model Pt complexes for platinum uridine green sulfate are the mono-, di-, and tetranuclear Pt−1-methyluracil complexes,[26−29] which, however, lack the ribose part. The tetranuclear *cis*-diammineplatinum−1-methyluracil blue[28] was the first structurally characterized paramagnetic platinum pyrimidine blue. Some of the mono- and dinuclear Pt complexes with 1-methyluracil are biologically active,[30] but diamagnetic and colorless or yellow.

The biologically inactive platinum uridine blue sulfate was studied earlier by AWAXS.[25] Even though only Pt has a suitable absorption edge for the measurement and the atomic fraction of Pt is only 0.023, an approximative Pt−Pt partial

† Department of Physics, University of Helsinki.
‡ Department of Chemistry, University of Helsinki.
§ Stanford Synchrotron Radiation Laboratory.
⊗ Abstract published in *Advance ACS Abstracts,* October 15, 1997.

(1) Rosenberg, B. *Nature* **1969**, *222*, 385. Rosenberg, B.; Van Camp, L.; Fisher, R. G.; Kansy S.; Peresie, H. J.; Davidson, J. P. Platinum−dioxopyrimidine complexes. US Pat 4419351, 1983.
(2) Davidson, J. P.; Faber, P. J.; Fischer, R. G.; Mansy, S.; Peresie, H. J.; Rosenberg, B.; VanCamp, L. *Cancer Chemother. Rep. Part 1,* **1975**, *59*, 287.
(3) Zaki, A. A.; McAuliffe, C. A.; Friedman, M. E.; Hill, W. E.; Kohl, H. H. *Inorg. Chim. Acta* **1983**, *69*, 93.
(4) Okuno, Y.; Tonosaki, K.; Inoue, T.; Yonemitsu, O.; Sasaki, T. *Chem. Lett.* **1986**, 1947.
(5) Shimura, T.; Tomohiro, T.; Laitalainen, T.; Moriyama, H.; Uemura, T.; Okuno, Y. *Chem. Pharm. Bull.* **1988**, *36*, 448.
(6) Serimaa, R.; Vahvaselkä, S.; Laitalainen, T.; Paakkari, T.; Oksanen, A. *J. Am. Chem. Soc.* **1993**, *115*, 10036.
(7) Laitalainen, T.; Serimaa, R.; Vahvaselkä, S.; Reunanen. A. *Inorg. Chim. Acta* **1996**, *248*, 121.
(8) Farrell, N. *Transition metal complexes as drugs and chemotherapeutic agents*; Kluwer Academic Publishers: The Netherlands, 1989, and references therein.
(9) Lippert, B. *Prog. Inorg. Chem.* **1989**, *37*, 1.
(10) Stetsenko, A. I.; Tikhonova, L. S. *Koord. Khim.* **1989**, *15*(7), 867.
(11) Barton, J. K.; Rabinowitz, H. N.; Szalda, D. J.; Lippard, S. J. *J. Am. Chem. Soc.* **1977**, *99*, 2827.
(12) Hollis, L. S.; Lippard, S. J. *Inorg. Chem.* **1983**, *22*, 2600.
(13) Sherman, S. E.; Gibson, D. A.; Wang, H.-J.; Lippard, S. J. *Science* **1985**, *230*, 412.
(14) Admiraal, G.; van der Veer, J. L.; de Graaff, R. A. G.; den Hartog, H. J.; Reedijk, J. *J. Am. Chem. Soc.* **1987**, *109*, 592.
(15) Iwamoto, M.; Mukundan, S. Jr.; Marzilli, L. G. *J. Am. Chem. Soc.* **1994**, *116*, 6238.
(16) Elmroth, S. K. C.; Lippard, S. J. *J. Am. Chem. Soc.* **1994**, *116*, 3633.
(17) Dunham, S. U.; Lippard, S. J. *J. Am. Chem. Soc.* **1995**, *117*, 10702.
(18) Takahara, P. M.; Rosenzweig, A. C.; Frederik, C. A.; Lippard, S. J. *Nature* **1995**, *377*, 649.
(19) Farrell, N.; Appleton, T. G.; Qu, Y.; Roberts, J. D.; Soeares Fontes, A. P.; Skov, K. A.; Wu, P.; Zou, Y. *Biochemistry* **1995**, *34*, 15480.
(20) Teo, B. K.; Kijima, K.; Bau, J. R. *J. Am. Chem. Soc.* **1978**, *100*, 621.
(21) Hitchcock A. P.; Lock C. J. L.; Lippert B. *Inorg. Chim. Acta* **1986**, *124*, 101.
(22) Laurent, M. P.; Biscoe, J.; Patterson. H. H. *J. Am. Chem. Soc.* **1980**, *102*, 6575.
(23) Soules, R.; Mosset, A.; Laurent, J.-P.; Castan, P.; Bernadinelli, G.; Delamar, M. *Inorg. Chim. Acta* **1989**, *155*, 105.
(24) Korsunsky, V. I.; Muraveiskaja, G. S.; Sidorov, A. A. *Inorg. Chim. Acta* **1991**, *187*, 23. Korsunskii, V. I.; Muraveiskaja, G. S.; Abashkin, V. E.; Fomina, I. G. *Russ. J. Inorg. Chem.* **1992**, *37*, 1042.
(25) Serimaa, R.; Eteläniemi, V.; Serimaa, O.; Laitalainen, T.; Bienenstock, A. *J. Appl. Crystallogr.* **1996**, *29*, 390.
(26) Dieter, I.; Lippert, B.; Schollhorn, H.; Thewalt, U. *Z. Naturforsch., Teil B* **1990**, *45*, 731. Neugebauer, D.; Lippert, B. *J. Am. Chem. Soc.* **1982**, *104*, 6596. Schollhorn, H.; Thewalt, U.; Lippert, B. *J. Am. Chem. Soc.* **1989**, *111*, 7213.
(27) Faggiani, R.; Lock, C. J. L.; Pollock, R. J.; Rosenberg, B.; Turner, G. *Inorg. Chem.* **1981**, *20*, 804. Lippert, B.; Neugebauer, D.; Raudushl, G. *Inorg. Chim. Acta* **1983**, *78*, 161. Lippert, B.; Schollhorn, H.; Thewalt, U. *J. Am. Chem. Soc.* **1986**, *108*, 525. Schollhorn, H.; Eisermann, P.; Thewalt, U.; Lippert, B. *Inorg. Chem.* **1986**, *25*, 407.
(28) Masharak, P. K.; Williams, I. D.; Lippard, S. J. *J. Am. Chem. Soc.* **1984**, *106*, 6428.
(29) O'Halloran, T. V.; Mascharak, P. K.; Williams, I. D.; Roberts, M. M.; Lippard, S. J. *Inorg. Chem.* **1987**, *26*, 1261.
(30) Woollins, J. D.; Rosenberg, B. J. *Inorg. Biochem.* **1983**, *19*, 41.

S0020-1669(96)01175-5 CCC: $14.00

structure factor was extracted by means of the Tikhonov regularization method. From the Pt−Pt partial radial distribution function it was concluded that the major Pt complexes are dinuclear. The biologically active platinum uridine green sulfate was found to exist as mono- and dinuclear Pt complexes in aqueous solution according to earlier small-angle X-ray scattering and nuclear magnetic resonance studies.[7,31]

2. Experimental Section

K_2PtCl_4 was obtained from Johnson Matthey, uridine from Sigma, and Ag_2SO_4 from Pfalz-Bauer. KI and H_2SO_4 were from BDH, TSK TOYOPEARL was from TosoHaas, acetone was from Labscan, and NH_3 and H_2O_2 Suprapur were from Merck. Deionized water was used in syntheses. Microanalysis is by H. Kolbe, Mikroanalytisches Laboratorium, Germany. VIS spectra were taken from aqueous solutions by means of a Shimadzu UV-200 double-beam spectrometer, and IR spectra of KBr pellets were obtained from a Biorad FTS-7 FTIR spectrometer. $[Pt(NH_3)_2(H_2O)_2]SO_4$ was synthesized according to the method of Dhara.[32]

For the preparation of platinum uridine green sulfate, a mixture of $[Pt(NH_3)_2(H_2\ O)_2]SO_4$ (70 mL, 7.00 mmol), uridine (1.7094 g, 7.00 mmol), and hydrogen peroxide (134 μL, 30%) was heated in a transparent flask in an oil bath at 52−54 °C for 2 h under an Ar atmosphere to give a green solution. The mixture was stirred for an additional 2 h at room temperature. The product was purified by gel filtration, and the green eluate was allowed to drop directly into a 10-fold amount of acetone. The precipitation was finalized at 8 °C during 12 h. Then the product was filtered with a sintered-glass funnel (G4) and dried under vacuum (1.33 Pa) for 12 h to give a green powder, 2.22 g (69.3% when based on Pt). The product for elemental analysis was synthesized in the same way. Elemental anal. Found: C, 15.02; H, 3.43; N, 9.22; S, 4.68; Pt, 42.63. VIS (H_2O): λ_{max} 730 nm. IR (KBr): 1625 cm^{-1} (C═O).

2.1. AWAXS Measurements. The AWAXS measurements were carried out at the Stanford Synchrotron Radiation Laboratory on wiggler beamline 4-3 utilizing a Si(111) double-crystal incident beam monochromator and a two-circle diffractometer in the symmetrical reflection mode. The sample was a 3 mm thick pressed pellet with an area of 10 × 40 mm^2. The parasitic scattering was reduced using He paths, but the sample itself was at normal atmosphere. The scattered intensity was measured in step−scan mode with a high-purity Ge solid state detector. The intensity of the primary beam was monitored by a scintillation counter (NaI). The intensity curve was measured in three parts, the accumulation time being increased for each part to collect more than 100 000 counts per point. The range of k was 0.3−10 $Å^{-1}$, and the steps were 0.05 $Å^{-1}$ ($k = (4\pi/\lambda)\sin\theta$ is the magnitude of the scattering vector, 2θ is the scattering angle, and λ is the wavelength). A total scan took 7 h. The employed photon energies of 10.6, 11.3, and 11.5 keV were below the Pt L_{III} absorption edge (11.564 keV). One measurement was performed without a sample to take parasitic scattering into account.

The experimental intensity curves were corrected for absorption and normalized to absolute scale with the large-angle method. Normalization involved determination and subtraction of fluorescence in the data and subtraction of the calculated Compton intensity.[33] The energy-independent atomic form factors and incoherent scattering functions were taken from *International Tables for X-ray Crystallography*.[34] Anomalous scattering factors (Table 1), evaluated from experimental X-ray absorption coefficients using the Kramers−Kronig dispersion relation, were used in the data analysis.

2.2. EXAFS Measurements. Transmission EXAFS studies were performed at Brookhaven National Laboratory at beamline X23A2. The synchrotron light was monochromatized using a double-crystal Si(220) monochromator with an energy resolution of about 5 eV. The measurement was repeated four times, the accumulation time increasing with the wave number k. The standards were elemental Pt and α-PtO_2. The jump in the optical thickness at the absorption edge was 1.0−1.3. At the high-energy side the optical thickness was 2−2.5. The samples, cooled to N_2 (liquid) temperature, were pressed to 2 mm thick pellets, which contained 50 mg of Pt green and 100 mg of twice-sublimed adamantane (Fluka AG).

Table 1. Anomalous Scattering Factors, Determined from EXAFS Data

energy (keV)	f'	f''
11.5	−13.10	3.91
11.3	−10.30	4.03
10.6	−7.46	4.46

The data were analyzed using the EXCURV90 program.[35] The constant imaginary potential ("vpi") and the reduction factor ("afac") were estimated using standards.

3. Solving Partial Structure Factors from AWAXS Data

The coherently scattered intensity, $I(E,k)$, can be written in terms of the partial structure factors $S_{\alpha\beta}$ as follows:[36]

$$I(E,k) = \sum_{\alpha} w_\alpha f_\alpha^*(E,k)\, f_\alpha(E,k) + \sum_{\alpha}\sum_{\beta} w_\alpha f_\alpha^*(E,k)\, f_\beta(E,k)\, S_{\alpha\beta}(k) \quad (1)$$

where w_α is the atomic fraction of the component α and $f_\alpha(E,k)$ is the scattering factor, which depends on the photon energy E and the magnitude of the scattering vector k. The first term, $\langle f^2\rangle = \sum_\alpha w_\alpha f_\alpha^*(E,k)\, f_\alpha(E,k)$, represents the coherent independent scattering.

The total structure factor (TSF) (eq 2), which is a weighted sum of all partial structure factors (PSFs), is calculated from the experimental coherently scattered intensity curve. From the TSF are obtained the total radial distribution function (RDF) (eq 3) and the function $\Delta\mathrm{RDF} = \mathrm{RDF}(r) - 4\pi r^2\rho_0$.

$$\mathrm{TSF}(E,k) = \frac{I(E,k) - \langle f^2(E,k)\rangle}{\langle f(E,k)\rangle^2} \quad (2)$$

$$\mathrm{RDF}(r) = 4\pi r^2\rho_0 + \frac{2r}{\pi}\int_0^\infty k\ \mathrm{TSF}(E,k)\sin kr\ \mathrm{d}k \quad (3)$$

The differential structure factors were calculated as

$$\mathrm{DSF}_{ij}(k) = \frac{I(E_i,k) - I(E_j,k) - (\langle f(E_i,k)^2\rangle - \langle f(E_j,k)^2\rangle)}{\langle f(E_i,k)\rangle^2 - \langle f(E_j,k)\rangle^2} \quad (4)$$

The photon energies E_i, $i = 1, 2, \ldots$, were chosen below the absorption edge of Pt. Because the scattering factors of the other elements (H, C, N, O, S) do not change markedly at these energies, the DSF will be approximately a weighted sum of only those partial structure factors $S_{\alpha\beta}(k)$ that involve Pt. The differential distribution function, DDF(r), was calculated as a Fourier transform of the differential structure factor.

Unfortunately the problem of solving PSFs from AWAXS data is ill-posed. In this case only an approximative regularized Pt−Pt PSF is obtained. To extract the experimental Pt−Pt PSF from the set of intensity curves the same regularization procedure is used as for platinum uridine blue:[25] The Pt complex is considered as a two-component system of Pt (denoted below by component α) and other elements H, C, N, O, and S lumped together (component β).

(31) Niskanen, E.; et al. To be published.
(32) Dhara, S. C. *Indian J. Chem.* **1970**, *8*, 193.
(33) Fuoss, P. H.; Eisenberg, P.; Warburton, W. K.; Bienenstock A. *Phys. Rev. Lett.* **1981**, *46*, 1537.
(34) *International Tables for X-ray Crystallography*; The Kynoch Press: Birmingham, England, 1974.
(35) SERC Daresbury Laboratory program EXCURV90; Binstead, N.; Gurman, S. J.; Campbell, J. W.; 1990.
(36) Keating, D. T. *J. Appl. Phys.* **1963**, *34*, 923.

The set of equations is of the form $y = Ax$, where the column matrix $x = \{S_{\alpha\beta}\}$ represents the PSFs to be determined. The matrix A is the coefficient matrix, which depends on the scattering factors, $f(E,k)$, and atomic fractions, w_α. The column matrix y is the input data, in this case the experimental intensities $I(E,k)$ from which $\langle f^2 \rangle$ is subtracted. This ill-conditioned set of linear equations, $y = Ax$, was solved by means of the Tikhonov regularization technique. Here the regularized least-squares functional is

$$||y - Ax||_2^S + \lambda ||x - x_M||_B^2 \quad (5)$$

where λ is the regularization factor, x_M a center vector (initial estimate), B a regularizing operator (or matrix), and S a weighting matrix. The notation $||z||_C^2 = \langle z|Cz \rangle$ denotes the norm of the vector z with respect to the inner product defined by the positive hermitian operator C.

The regularization factor, λ, controls the "strength" of the regularization. For more universality it is scaled as follows:

$$\lambda = \tilde{\lambda} \frac{||A||_S^2}{||B||} \quad (6)$$

The regularization term, $||x - x_M||_B^2$, is a constraint to minimize the difference between the solution, x, and the initial estimate, x_M. The center vector, x_M, is a known vector, which approximates the true solution, x_T. The inverse of the covariance matrix, cov(y), of the data, y, is used as the weighting matrix; $S = \text{cov}(y)^{-1}/m$, where m is the dimension of the target space. With this choice the optimal residual, $||y - Ax||_S^2$, is on average about unity.[37]

These sets of equations were solved separately at each k, and the regularization functional was

$$||x||_B^2 = \sum_{i=1}^{K} \alpha_i ||x_i||_{b_i}^2$$

where the regularization matrices b_i, $i = 1, ..., 3$, were the norm of the solution vector x_λ, the first differences of x_λ, and the second differences of x_λ with respect to its component indices and α_i were set to 1. The regularization parameter λ of 0.0001 was used. The initial center vector components x_{M1} and x_{M3} for $S_{\alpha\alpha}$ and $S_{\beta\beta}$, respectively, were set equal to 0, while x_{M2} for $S_{\alpha\beta}$ was a simulated PSF $S_{\alpha\beta}$ of a unit containing one platinum, and four oxygens at the distance of 2 Å from the platinum, on the basis of the interpretation of the first maximum of the RDF.

Finally, the partial distribution function PDF(r) and the function $\Delta\text{PDF} = P_{\alpha\alpha} - 4\pi r^2 w_\alpha \rho_0$ were calculated as a Fourier transform of the partial structure factor.

4. Results

The results will be given in following order: AWAXS data are analyzed to get an experimental average Pt−Pt coordination number at about 3 Å. Then several model Pt structures are constructed on the basis of the structures of analogous crystalline Pt complexes, and their ΔRDFs, ΔDDFs, and ΔPDFs are compared with the experimental ones. Finally the most plausible models chosen on the basis of AWAXS data are compared with EXAFS data.

4.1. AWAXS Results. The total (TSF) and the differential (DSF) structure factors are shown in Figure 1. The ΔRDF (11.5 keV), the ΔDDF (11.5, 10.6 keV) and ΔPDF (11.5, 11.3, 10.6 keV) are compared in Figure 2. The positions of the most pronounced maxima of the Pt−Pt ΔPDF, the ΔRDF, and the ΔDDF and the coordination numbers at 2 and 3 Å, which were determined as areas of the maxima of the RDF, the DDF, and the Pt−Pt PDF, are given in Table 2. The precisions of the positions of the maxima of ΔRDF, ΔDDF, and ΔPDF are ±0.05, ±0.05, and ±0.1 Å, respectively, and the precisions of the coordination numbers from the RDF, DDF, and PDF are 10%, 15%, and 30%, respectively, since the maxima are not well resolved and the largest k used for calculation of the PDF was only 8.5 Å^{-1}. The statistical precision of the intensity curves was better than 0.3%, which means that the ΔRDF is (statistically) reasonably accurate at least up to 15 Å and the

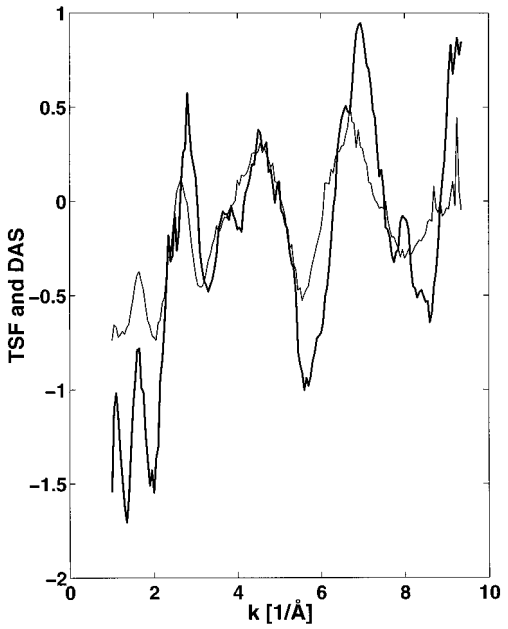

Figure 1. Experimental total (thin line) and differential structure factors (thick line) of platinum uridine green sulfate.

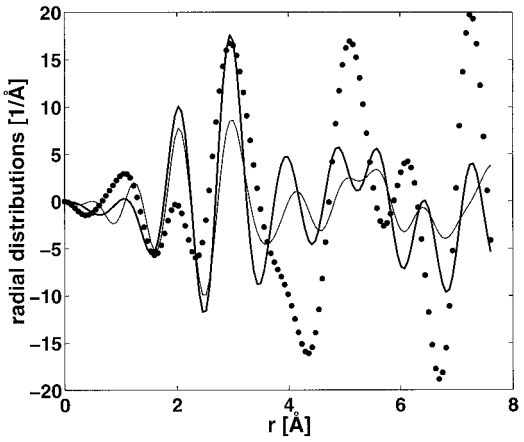

Figure 2. Experimental ΔRDF (thin line), ΔDDF (thick line), and ΔPDF/w_α (dotted line) for platinum uridine green sulfate.

Table 2. Positions of the Most Prominent Maxima (Å) of the ΔRDF and ΔDDF Compared with the Estimated Pt−Pt Distances Determined from the Pt−Pt PDF[a]

	distances (Å)						coord no.	
							at 2 Å	at 3 Å
RDF	2.0	3.03	4.2	5.1	5.6	7.6	4.8	10
DDF	2.0	3.0	4.0	4.9	5.6	7.3	6.0	14
PDF		2.95		5.1		7.3		0.5

[a] The average coordination numbers at about 2 and 3 Å are also given.

(37) Tikhonov, A. N.; Arsenin, V. Ya. *Solution of Ill-Posed Problems*; Wiley: New York, 1977.

ΔDDF up to about 10 Å.[38] On the basis of the simulations and the fact that the experimental data may contain systematic errors, we estimate that the solved experimental Pt−Pt PDF is reasonably accurate only up to about 6 Å.

The interpretation of the results is based on comparison of the functions ΔPDF, ΔRDF, and ΔDDF. The Pt−Pt distances are identified as the positions of the maxima of the Pt−Pt ΔPDF and also are identified by comparing the functions ΔRDF and ΔDDF. The approximate weight of the Pt−Pt PSF is 3.7 in the TSF and 12.5 in the DSF, and those of the Pt−N and Pt−O PSFs are about 0.8 and 1.0 in the TSF and DSF, respectively. Because the weight of the Pt−Pt PSF is larger in the DSF than in the TSF, the maxima arising from Pt−Pt distances are more intensive in the ΔDDF than in the ΔRDF.

The ΔRDF and ΔDDF contain maxima at about 3 and 5 Å. The fact that they are more intensive in the ΔDDF than in the ΔRDF indicates that they arise from Pt−Pt distances. Because the maximum at 7.3 Å is not clearly visible in the ΔRDF and ΔDDF, it is believed that, due to the statistical errors, its intensity in the Pt−Pt ΔPDF is too large. The average Pt−Pt distances, determined from the positions of the maxima of the ΔPDF, are thus 3.0(1), 5.1(1), and 7.3(1) Å.

The maximum at 2 Å, which is present in the ΔRDF and ΔDDF but is not significant in the ΔPDF, arises mainly from Pt−N and Pt−O distances. On the basis of the structures of the crystalline model Pt complexes,[12,29] the coordination number of the DDF at 2 Å is the average Pt−N,O coordination number weighted with the factor

$$\frac{[f'_\alpha(E_i) - f'_\alpha(E_j)](f_\beta + f^*_\beta)w_\alpha}{\langle f(E_i)\rangle^2 - \langle f(E_j)\rangle^2}$$

where α denotes Pt and β N and O. By inserting the atomic fraction of Pt of about 0.03 and $(f_\beta + f^*_\beta)/2$ between 7.25 and 8 depending on the amount of N and O in the first coordination sphere of Pt, the weighting factor will be between 1.3 and 1.4 and the average Pt−N,O coordination number between 4.5 and 4.3. The maximum that exists in the ΔRDF and ΔDDF at about 4 Å but not in the ΔPDF arises mainly from Pt−N,O,C distances. Its contribution is increased in the ΔDDF, which might indicate that there are a small number of Pt−Pt distances of about 4 Å. However, the precision of the experimental Pt−Pt PDF is not good enough for verifying this.

The first maximum of the RDF at 1.4 Å arises from C−C, C−N, C−O, and N−O distances, but other distances between these light elements cannot be distinguished from the ΔRDF and ΔDDF because their contribution to the total structure factor is small. The features of the DDF and PDF below 2 Å are "Fourier ripples".

4.2. Model Pt Structures. Hollis and Lippard followed the formation of Pt complexes of *cis*-diammineplatinum(II) with a bridging α-pyridonate ligand.[12] They showed that when the *cis*-$[(NH_3)_2Pt(H_2O)_2]^{2+}$ reacted with α-pyridone, a mixture including mononuclear Pt complexes, unreacted *cis*-$[(NH_3)_2Pt(H_2O)_2]^{2+}$ complexes, and hydroxo-bridged dimers $[(NH_3)_2Pt(OH)Pt(NH_3)_2]^{2+}$ was formed. The dinuclear Pt−α-pyridone complex became the dominating species only after several hours. Product selectivity was obtained by pH control. We suggest on the basis of elemental analysis that platinum uridine green sulfate contains *cis*-$[(NH_3)_2Pt(H_2O)_2]^{2+}$ in the solid state. Our extensive ^{15}N-labeled multinuclear NMR studies[31] indicate that it is present also in the aqueous solution of Pt−uridine green sulfate.

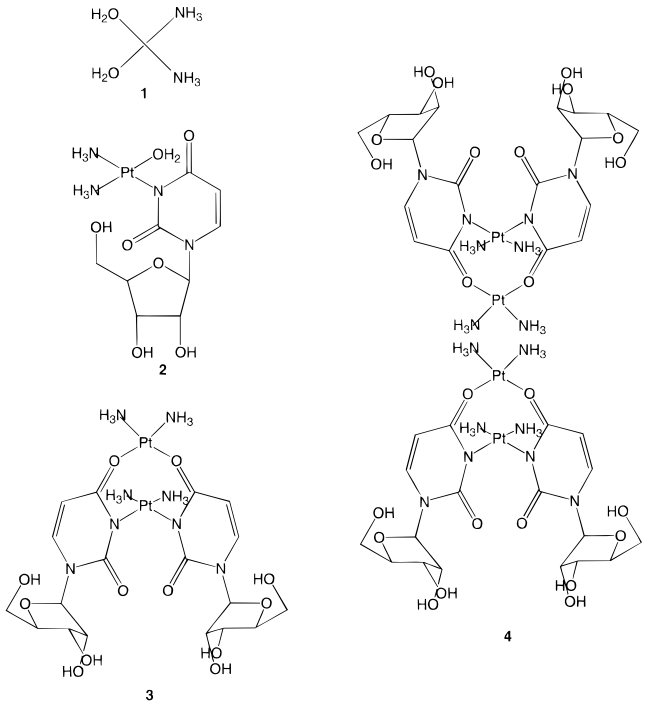

Figure 3. Assumed mononuclear (**1** and **2**), dinuclear (**3**), and tetranuclear (**4**) Pt−uridine complexes.

No unit cell for Pt−uridine green can be determined from AWAXS and EXAFS data due to its amorphous nature. To simulate the experimental data we have built, on the basis of the crystal structures of Pt−1-methyluracil complexes[27,29] and uridine,[39] the following hypothetical Pt complexes, (see Figure 3): mononuclear *cis*-$[(NH_3)_2Pt(H_2O)_2]^{2+}$ (**1**), mononuclear $[Pt(NH_3)_2(uridine)(H_2O)]^{q+}$ complex, $q = 1, 2$ (**2**); dinuclear $[Pt^{II}]_2$ complex $[Pt_2(NH_3)_4(uridine)_2]^{2+}$ (**3**); and tetranuclear $[Pt^{II}]_4$ or $[Pt^{II}]_3[Pt^{III}]$ complex $[Pt_4(NH_3)_8(uridine)_4]^{q+}$, $q = 4, 5$ (**4**).

A crystalline Pt complex of type **2** has been synthesized with, e.g., 1-methylcytosine,[40] but not with 1-methyluracil. Crystalline Pt−1-methyluracil complexes of types **3** and **4** with several Pt oxidation states are known.[27,29] The experimental Pt−Pt distance of 3 Å is in the range of typical intramolecular Pt−Pt distances of $[Pt^{II}]_2$ complexes. More oxidized dinuclear Pt complexes than **3**, like $Pt^{II}Pt^{III}$ and $[Pt^{III}]_2$, and tetranuclear Pt complexes than **4**, like $[Pt^{II}]_2[Pt^{III}]_2$, $Pt^{II}[Pt^{III}]_3$, and $[Pt^{II}]_4$, are excluded, since their intramolecular Pt−Pt distances are expected to be shorter[8] than the experimental result, 3 Å. Furthermore, no crystalline $Pt^{III}Pt^{II}$ complexes are known but their formation by electrochemical oxidation[41] and as intermediates in Ce(IV) oxidation of $[Pt^{II}]_2$ complexes[42] has been reported.

The Pt complexes **2**−**4** were built either by joining the Pt complex **1** with uridine or by replacing the methyl group of 1-methyluracil by the ribose part of uridine. The platinum positions were optimized to fit the experimental ΔRDF measured with 17.4 keV.[6] The counterion SO_4^{2-} is included in the scattering units, but its contribution to the RDF and DDF is small.

The heights of the maxima of the ΔDDF and ΔRDF at 3 Å depend on the Pt nuclearity of the sample. For example, Figure

(38) Thijsse, B. J. *J. Appl. Crystallogr.* **1984**, *17*, 61.
(39) Green, E. A.; Rosenstein, R. D.; Shiono, R.; Abraham, D. J.; Trus, B. L.; Marsg, R. E. *Acta Crystallogr., Sect. B* **1975**, *31*, 102.
(40) Britten, J. F.; Lippert, B.; Lock, J. L.; Pilon, F. *Inorg. Chem.* **1981**, *21*, 1936.
(41) Ramstad, T.; Woollins, J. D.; Weaver, M. J. *Inorg. Chim. Acta* **1986**, *124*, 187.
(42) Peilert, M.; Erxleben, A.; Lippert, B. *Z. Anorg. Allg. Chem.* **1996**, *622*, 267.

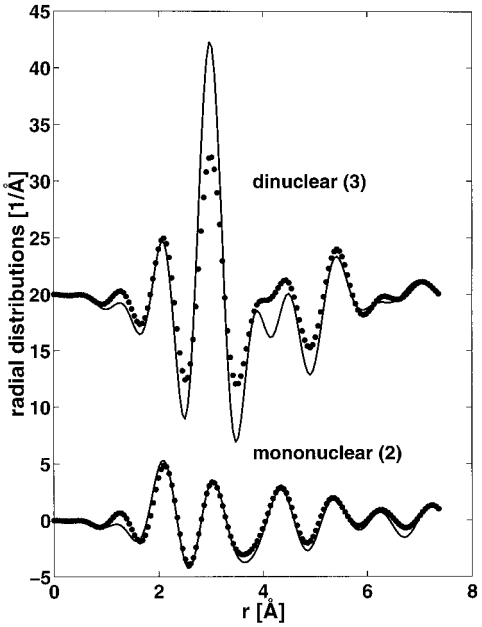

Figure 4. Calculated ΔRDF (dotted line) and ΔDDF (solid line) of the hypothetical mononuclear (**2**) and dinuclear (**3**) Pt complexes.

Table 3. Calculated S/Pt and Uridine/Pt Ratios and the Ratio of the Areas of the Maxima at 3 Å of the DDF and RDF, CN(DDF)/CN(RDF), as a Function of the Composition of a Hypothetical Mixture of the Pt Complexes **1**−**4**

fraction of Pt complexes in the mixture				ratio		
mono		di	tetra			
(**1**)	(**2**)	(**3**)	(**4**)	S/Pt	uridine/Pt	CN(DDF)/CN(RDF)
1				1.0	1	1.0
	1			0.5−1.0	1	1.0
		1		0.5	1	1.7
			1	0.5−0.7	1	2.0
$^1/_3$	$^1/_3$	$^1/_3$		0.6−0.9	0.7	1.4
$^2/_5$	$^2/_5$		$^1/_5$	0.7−0.9	0.7	1.4

4 shows the simulated ΔRDFs and ΔDDFs of the mono- and dinuclear Pt complexes **2** and **3**. The heights of the maxima of the ΔDDF and ΔRDF at 3 Å are nearly equal for the mononuclear Pt complex **2**, but for the dinuclear complex **3** that of the ΔDDF is considerably higher. The experimental ratio of the areas of the 3 Å maximum of the DDF and RDF, CN(DDF)/CN(RDF), is 1.4(2) (Table 3). For the mononuclear Pt complex **2** a too low ratio is obtained, and for the di- and tetranuclear Pt complexes **3** and **4** too high ratios are obtained.

Several model scattering units whose Pt nuclearity and the CN(DDF)/CN(RDF) ratio are in accord with the AWAXS data may be constructed by varying the shares of the Pt complexes **1**−**4**. Table 3 gives the CN(DDF)/CN(RDF), S/Pt, and uridine/Pt ratios for a mixture of mono- and dinuclear Pt complexes and a mixture of mono- and tetranuclear Pt complexes. In both cases a portion of the mononuclear Pt complexes was assumed to be of type **1**, and their share was chosen to fit the experimental uridine/Pt ratio of 0.6. The fractions of di- and tetranuclear Pt complexes were chosen to fit the Pt−Pt coordination number at 3 Å. These models agree also with the experimental S/Pt ratio of Pt−uridine green sulfate of 0.7.

The obtained Pt−Pt distances of 5.1 and 7.6 Å (Table 2) do not agree with a linear Pt chain similar to that of platinum 1-methyluracil blue.[29] Since the predicted share of 20% of Pt complex **4** for the mixture of Pt complexes **1**, **2**, and **4** would cause extra maxima in the ΔRDF, it is assumed that the share of tetranuclear Pt complex **4** is small.

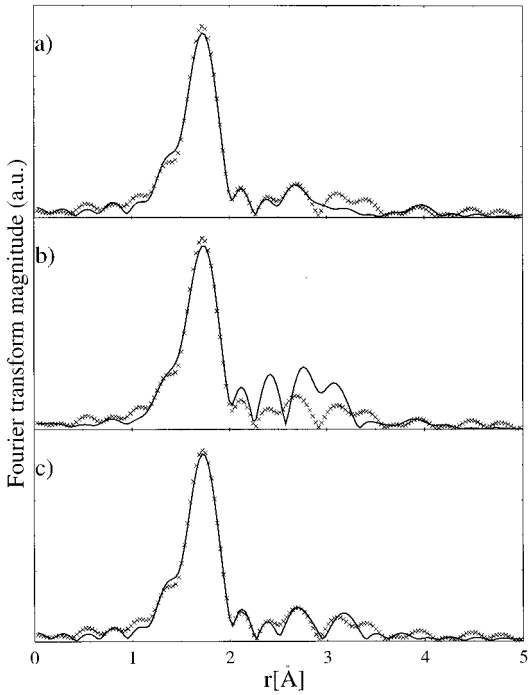

Figure 5. Fourier transform |FT($k^3\chi$)| (the radial distribution function that is not corrected for the phase shifts) from EXAFS data of platinum uridine green sulfate (x-marks) with models (solid line): (a) mononuclear model (**2**), (b) dinuclear model (**3**), (c) mixture model.

Table 4. Nearest Neighbors of an Average Pt Atom in Models **1**−**4**

		coord no.			
distance from Pt (Å)		**1**	**2**	**3**	**4**
2.0	Pt−N, Pt−O	4	4	4	4
2.7−3.0	Pt−C, Pt−O		4	3	4
2.9−3.1	Pt−Pt			1	1.5
3.0−3.3	Pt−N			2	3

4.3. EXAFS Studies. The Fourier transform |FT($k^3\chi$)| (the radial distribution function that is not corrected for the phase shift) of the EXAFS oscillation χ weighted by k^3 is shown in Figure 5. The radial distribution function contains one pronounced maximum arising from the first coordination shell of Pt and only small peaks at the distances of 2.3−3.2 Å, but their positions were the same in each scan.

The nearest neighbors of an average Pt atom in the models **1**−**4** are given in Table 4. The first coordination shell of all models (**1**−**4**) consists of four O and N atoms at a distance of 2 Å from a Pt atom. The Pt atom of model **1** has no further neighbors, and those of the models **2**−**4** have 4−7 O, N, and C atoms at distances of 2.3−3.2 Å.

It is assumed that the first coordination shell of platinum contains both nitrogen and oxygen atoms, but in EXAFS data these two elements are indistinguishable. The average Pt−N, Pt−O coordination number is determined by inverse Fourier transforming the range 1.1−2.3 Å, of the function FT($k^3\chi$). The refinements to the Fourier filtered data gave 4−4.5 atoms depending on whether only an oxygen or a nitrogen shell was fitted. This agrees well with the AWAXS result of 4.3−4.5 atoms. The refined average Pt−N, Pt−N distance is 2.02(2) Å, and the Debye−Waller factor ($2\sigma^2$) is 0.0044(3) Å^2.

Each maximum in the range 2.3−3.2 Å, was inverse Fourier transformed in order to identify the maxima arising from Pt−Pt distances. A Pt−Pt distance gives an oscillation whose amplitude increases with k whereas Pt−O, Pt−N, and Pt−C distances give oscillations whose amplitude decreases with k.

It was found out that a maximum arises from a Pt−Pt distance and the rest from Pt−C, Pt−N, and Pt−O distances. No Pt−S distance is evidenced in this range. Refinements of the Fourier filtered data predicted a smaller Pt−Pt coordination number than 0.5. It may be too small, since when fitting only one shell to a narrowedly filtered maximum, the cancellation effects of close-by Pt−C, Pt−N, and Pt−O distances on the Pt−Pt coordination number are not taken into account.

Thus multishell refinements were performed, too. The inverse Fourier transformed range was 1.1−3.2 Å. The shells were chosen on the basis of models **2**−**4**. Unfortunately, for Pt−uridine green sulfate the fitting results will not be unique because of the large number of coordination shells. Three shells, Pt...C, Pt...N, and Pt...Pt, at a distance of about 3 Å and the first coordination shell at a distance of about 2 Å were included, because the elements C, N, and O are indistinguishable in the refinement. The distances and the coordination numbers were varied, but the Debye−Waller factors were fixed to 0.0044 (C, N, and O) and 0.007 Å^2 (Pt). Because the Debye−Waller factor for Pt is based on EXAFS data of Pt foil, the obtained Pt−Pt coordination number may be too small.

The refinement gave a Pt−Pt coordination number of 0.6 and a Pt−Pt distance of 2.98(1) Å, which are in accord with a mixture where the major components are mono- and dinuclear Pt complexes. The simulated EXAFS data of this mixture model and of models **2** and **3** are compared with the raw experimental data in Figure 5. Figure 5 shows that the mixture model agrees with the experimental data in the whole range 0−3.2 Å. The mononuclear model **2** agrees quite well with the experimental data at distances smaller than 2.8 Å, but at larger distances its radial distribution function does not include any maxima, which is not in accord with the experimental data. The dinuclear model **3** disagrees with the experimental EXAFS data yielding too large maxima in the range 2.3−3.2 Å which is in accord with AWAXS results.

5. Discussion

The main result of this AWAXS and EXAFS study is that the shortest Pt−Pt distance of Pt−uridine green sulfate is about 3 Å with a coordination number of about $^1/_2$. This low value for the average Pt nuclearity excludes both the polymeric mixture,[8,43] and the homogeneous polynuclear Pt complex,[5,44] which have been suggested earlier as structures of amorphous Pt blues and greens. Accordingly, also the suggested explanations for the biological activity of Pt−pyrimidine greens need reconsideration.

On the basis of AWAXS, EXAFS, and elemental analysis results it is proposed that Pt−uridine green sulfate is a mixture of mono-, di-, and tetranuclear Pt complexes **1**−**4** where the amount of **4** is smaller than 20%. This composition explains the low uridine/Pt ratio, paramagnetism, color, and catalase activity.

EXAFS turned out to be a good method to study the structure of the first coordination shell of platinum. The presence of a Pt−Pt distance of about 3 Å could also be verified by EXAFS, but the coordination number could not be determined unambiguously. A more reliable value for the Pt nuclearity was obtained by the AWAXS method. Even though the problem of solving PSFs from a set of intensity curves measured in the vicinity of the Pt L_{III} absorption edge is ill-conditioned, an approximative Pt−Pt partial structure factor was obtained from the AWAXS data. The use of the regularization technique minimized problems related to ill-conditioning and statistical errors in the data. The experimental Pt−Pt PDF was consistent with the total RDF obtained with one and the DDF obtained with two photon energies.

The AWAXS, EXAFS, and earlier WAXS results[6,25] of both the biologically active platinum uridine green sulfate and inactive platinum uridine blue sulfate can be explained in terms of the mixture of Pt complexes **1**−**4**. However, the X-ray scattering results reveal differences in the intermolecular order between platinum uridine green and blue sulfates. For both of them about the same Pt−Pt distance of 3 Å was obtained, which indicates that they contain dinuclear Pt complexes **3**. The RDF of platinum uridine blue sulfate obtained with Mo Kα radiation included also a maximum at 2.6 Å, which is not present in the RDF of platinum uridine green sulfate.[6,25] It was suggested[25] that the maximum at 2.6 Å arises from an intradinuclear Pt−Pt distance of a dinuclear $[Pt^{III}]_2$ units. According to the uridine/Pt ratio the amount of Pt complexes **1** is much smaller for platinum uridine blue (5%) than for platinum uridine green (30%) in the solid state.

The biological activity of the cancer drug cisplatin is explained by the formation of the Pt complex **1** in the cellular environment and its binding with DNA.[13] A similar mechanism is one possible explanation also for the biological activity of platinum uridine green sulfate. However, the presence of Pt complex **1** in the solid product is not considered as a reason for the antitumor activity of platinum uridine green sulfate since the products of hydrolysis of cisplatin have been reported to increase the nephrotoxicity and to decrease the antitumor activity.[45] AWAXS and EXAFS results[47] of the Pt greens synthesized with uridine derivatives studied previously by SAXS[7] and results of NMR experiments of the variously colored Pt−uridine complexes[31] will give further arguments about the relationships of the composition, the structure, and the antitumor activity of platinum nucleoside green sulfates.

6. Conclusion

The Pt−Pt coordination number of 0.5 at 3 Å excludes any homogeneous polynuclear Pt complex as the structure of platinum uridine green sulfate. The AWAXS, EXAFS, and elemental analysis results were interpreted in terms of a mixture of mono- and dinuclear major Pt complexes. The proposed composition is in accord with properties of Pt−uridine green sulfate. This work demonstrates the advantages of using both AWAXS and EXAFS methods for studying structures of complex amorphous materials. The study encourages especially the use of the AWAXS method to solve a specific partial structure factor of a multicomponent system even if the sample contains only one element with a suitable absorption edge for the measurement.

Acknowledgment. This research was supported by the Academy of Finland, the Neste Foundation, the Technology Development Centre, the University of Helsinki, and the Office of Basic Energy Sciences of the U.S. Department of Energy. The synchrotron radiation work was performed at SSRL, which is supported by the U.S. Department of Energy, Office of Basic Energy Sciences.

IC9611756

(43) Barton, J. K.; Caravana, C.; Lippard, S. J. *J. Am. Chem. Soc.* **1979**, *101*, 1269.
(44) Okada, T.; Shimura, T.; Okuno, H. *Inorg. Chim. Acta* **1990**, *178*, 13.
(45) Daley-Yates, P. T.; McBrien, D. C. H. *Biochem. Pharmacol.* **1984**, *33*, 3063. Andersson, A.; Hedenman, H.; Elfsson, B.; Ehrsson, H. *J. Pharm. Sci.* **1994**, *83*, 859.
(46) Bancroft, D. P.; Lepre, C. A.; Lippard, S. J. *J. Appl. Crystallogr.* **1990**, *112*, 6860.
(47) Serimaa, R.; Eteläniemi, V.; Paakkari, T.; Laitalainen, T.; Bienenstock, A. AWAXS Study of Amorphous Platinum Complexes. Activity Report 1992; Stanford Synchrotron Radiation Laboratory, Stanford University, Stanford, CA, 1992; pp 145−148.